Chapter V: A Comparison of the Antagonist Binding Sites of the Human Dopamine Receptors

Chapter V: A Comparison of the Antagonist Binding Sites of the Human Dopamine Receptors

Abstract:

The dopamine neurotransmitter and its receptors play a critical role in such diseases as Parkinson's and schizophrenia. A problem with developing drugs for such diseases is that there are five subtypes of dopamine receptors, only one of which should be affected for each disease. Since the binding sites are quite similar, it is difficult to design the subtype specific agonists and antagonists required for therapy with minimal side effects. This task has been particularly difficult since there are no crystal structures for any dopamine receptors or any closely related G-protein coupled receptors (GPCR) because of the difficulties in crystallizing these membrane-bound proteins.

We have previously reported the 3-D structure of the human D_2 dopamine receptor (hD_2DR), predicted from the primary sequence using *ab initio* theoretical and computational techniques.[1] This 3-D structure was validated by predicting the binding site and relative binding affinities of dopamine plus 3 known dopamine receptor agonists (antiparkinsonian) and 8 known antagonists (antipsychotic) in the hD_2DR receptor. Herein we report the homology structures for the other 4 subtypes of the human dopamine receptors based on the predicted structure of the hD_2DR, and utilize these homology structures to study the antagonist binding sites of clozapine and haloperidol to all 5 receptors. Our studies provide a quantitative, residue-by-residue, contribution of all 5 Å residues to antagonist binding, and provide insight into the receptors' ability to

differentiate between D_1 and D_2 specific ligands. The predicted structure and the homology structures of the remaining members provide insight into the modifications in the dopamine receptors that allow for differential binding of some ligands but non-discriminatory binding of others, and can be utilized in the design of receptor and subtype specific agonist therapies for maladies such as Parkinson's.

Introduction:

Biogenic amines (such as epinephrine, dopamine, norepinephrine, tryptophan, and serotonin) play an essential role in the central and peripheral nervous systems. These molecules exert their effects by binding to the extracellular surface of a GPCR, which causes changes that lead to activation of a G-protein on the intracellular surface, which in turn leads to a cascade of events in the cytoplasm. GPCRs consist of an extracellular amino terminus, an intracellular carboxy terminal region, and seven □-helical transmembrane (TM) domains. Three intracellular (IC) and three extracellular (EC) loops connect the seven transmembrane domains of the protein.

Dopamine, a catecholamine intermediate in the biosynthesis of epinephrine and norepinephrine, is a particularly well-studied biogenic amine, whose receptors are important targets for treating schizophrenia (antagonists to D_3)[2] and Parkinson's diseases (agonists to D_2)[3]. There are five known human Dopamine Receptors (DRs) with multiple isoforms for each.[4] These DRs are classified on the basis of their pharmacological characteristics into two subfamilies:

- D_1like: D_1 and D_5 show 82% sequence homology. These receptors have a short third intracellular loop (IC3) and a long carboxy terminus.
- D_2like: D_2, D_3, D_4 show 54 to 76% sequence homology (76% homology between D_2 and D_3 and 54% between D_2 and D_4). These receptors have a long IC3 loop and a short carboxy terminus.
- On the other hand the D_1 and D_2 DRs have a sequence homology of only 44%.

Mutational studies have indicated that the IC3 loop is directly involved in G-protein coupling[5], but it is unlikely that these length differences between D_1 and D_2 affect the interaction the binding of dopamine.

Since all five DR's are activated by the same endogenous ligand, dopamine, the binding sites of these receptors are expected to be quite similar. The similarity of elements in the binding site of the dopamine receptors creates a challenge to design agonists and antagonists specific to only one subtype of the DR's, with little or no cross reactivity with other subtypes and other GPCRs with high homology. This difficulty is exacerbated greatly by the lack of an experimental 3-D structure for any DR of any species. Indeed considering GPCRs from all forms of life, there is a single 3-D structure for bovine rhodopsin[6]. The experimental shortcomings are the result of the low expression levels of GPCRs and the difficulties associated with crystallizing a membrane bound protein. Some research groups have attempted to alleviate the problem by building homology models for the D_2DR based on the structure of bacteriorhodopsin[7], or bovine

rhodopsin[8]. Unfortunately, due to the low sequence similarity of 19% between the D_2DR and bovine rhodopsin, these homology models are not accurate enough to be used in design of subtype specific drugs. It must be noted, however, that homology models based on bovine rhodopsin have been invaluable tools in rationalizing the results of biochemical experiments; and, once refined using experimental data and distance restraints, these models could serve as coarse model for design of receptor specific drugs. The true shortcomings of the homology models arise in cases where little or no experimental data is available for refinement of the homology model.

Because sufficiently accurate experimental structures are not available, we have developed computational first principles methods to predict the three-dimensional structures of GPCRs (MembStruk) and to predict the binding site and energy for various ligands to these structures (HierDock). These methods have been validated on bovine rhodopsin[9], human β2-adrenergic receptor [10], and 10 mouse olfactory receptors [11]. Recently we provided and overview of the binding site of agonists and antagonists in the human dopamine D_2DR denoted as hD_2DR[1] predicted using these methods. In this paper, we utilize the previously reported structure of the hD_2DR as a template for homology modeling the other 4 subtypes of the human dopamine receptors to study the binding sites of the classic antagonists clozapine and haloperidol; from these comparative studies, we have gained great insight into the changes in the receptor that bring about the differential binding of ligands to each receptor. The residues involved in recognizing dopamine and their contributions to the binding energy are also described herein. The results from *ab initio* and homology model structures are in excellent agreement with the experimental

data on the binding sites and ligand affinities to the hD_xDR (where x=1, 2, 3, 4 or 5), validating these structures. In addition, we have gained new insights about the characteristics of these receptors and the modifications resulting in differential binding of ligands. Our results are likely to stimulate experiments and are useful for design of subtype specific ligands for dopamine receptors. The validation of the computational techniques for these well-characterized systems, allows for the use of these methods to be extended to other GPCR targets where little experimental information is known.

Materials and Methods:

Choice of forcefields (FF): All calculations for the protein used the DREIDING FF[12] with charges from CHARMM22[13] unless specified otherwise. The non-bond interactions were calculated using Cell Multipole Method[14] in MPSim[15]. The ligands were described with the DREIDING FF using Gasteiger charges[16]. For the lipids we used the DREIDING FF with QEq charges[17]. Some calculations were done in the vacuum (e.g., final optimization of receptor structure to approximate the low dielectric membrane environment). Most calculations treated the solvent (water) using the Analytical Volume Generalized Born (AVGB) approximation to Poisson-Boltzmann solvation model[18].

MembStruk Structure Prediction Method: The MembStruk procedure version MembStruk3.0 used to predict the three dimensional structure of hD_2DR is described in detail in *reference 9*. Here we detail the steps that are relevant to the prediction of hD_2DR. The various steps of the MembStruk procedure are as follows:

The seven TM boundaries of the hD_2DR were predicted using TM2ndS[9b] procedure. Twenty sequences of D_2DR across many species were aligned using multiple sequence alignment program CLUSTALW[19].

This alignment was used to predict the TM regions using TM2ndS. The predicted TM regions of the human D_2 dopamine receptor are shown in **Scheme 5-1**. It is seen that the seven TM helices in hD_2DR are of different length and also are different in length from the corresponding TM helices of rhodopsin. We built 7 canonical □-helices, and then constructed the TM seven helical barrel with the helical axes positioned based on the 7.5 Å three-dimensional density map of frog rhodopsin[20].

(a) We then performed optimization of the translational orientation of the canonical helices by using the hydrophobic center algorithm described in *reference 9*. The maximum hydrophobic centers of the seven helices are residue 17 for TM1, residue 13 for TM2, residue 11 for TM3, residue 11 for TM4, residue 13 for TM5, residue 15 for TM6 and residue 16 for TM7. These hydrophobic centers were fitted to a plane and thus an optimum of relative translational orientation of the helices was obtained.

(b) The rotational orientation of the canonical helices was also optimized using the multisequence hydrophobicity moments, of the middle third of each helix about their maximum hydrophobic center and were optimized based on energy. These

analyses yielded a clear consensus on which residues should contact the membrane and which should face the receptor interior.

(c) The canonical helices were optimized with NEIMO torsional dynamics[21] or Cartesian dynamics (described with the DREIDING FF and Charmm22 charges), for 500 ps at 300 K constant temperature and picked the minimum energy conformation from the dynamics. This step optimizes the kinks and bends in the helices.

(d) The helical bundle now has helices with bends and kinks. The rotational orientation of these non-canonical helices was further optimized using both the procedure in step c) followed by energy based optimization called "Rotmin" described in *reference 9*. Steps c), d) and f) is a part of systematic search algorithm for optimum translational and rotational orientation and these steps aid in getting over large barriers for structure optimization.

(e) The optimized TM barrel structure was then equilibrated by immersing it in a bilayer barrel of dilauroylphosphatidyl choline and the full system was optimized with rigid body quaternion molecular dynamics (MD), treating each molecule as a rigid body for 50 ps at constant temperature of 300 K using MPSim code.

(f) The interhelical loops were built using WHAT IF[22] and disulfide bonds were formed between Cys 107 in TM3 and Cys 182 in extracellular loop 2. This full system was then optimized with conjugate gradient minimization technique to 0.1kcal/mol/Å RMS in force.

Homology Structure Prediction Method: We utilized standard homology modeling techniques as described in *references 7-8* to build the 3-D models for the D_1, D_3, D_4 and D_5 subtypes of the human dopamine receptors using the predicted structure of the hD_2DR as the template.

Prediction of Ligand Binding Sites and Binding Energies:

Ligand Structure Preparation: Clozapine and haloperidol shown in **Figure 5-1** was built with chemdraw and the two dimensional structure was converted to three dimensional structures in cerius2. Hydrogens were added with Gasteiger charges assigned also using the concord software. We then minimized the potential energy of each ligand using conjugate gradients to a RMSD in force of 0.1kcal/mol/Å.

Function Prediction: HierDock protocol is a hierarchical strategy of ranging from coarse-grain docking to fine-grain optimization for docking ligands in proteins. This method has been tested for various GPCRs[9-11], membrane proteins[23] and globular proteins[24]. This protocol has been described in detail in these references. In here we use

the version of HierDock2.0 described in *reference 9a*. In brief the various steps of HierDock protocol version 2.0 is as follows:

The HierDock ligand screening protocol follows a hierarchical strategy for examining ligand binding conformations, and calculating their binding energies. The steps are as follows:

1) First we carry out a coarse grain docking procedure to generate a set of conformations for ligand binding in the receptor. Here we use Dock 4.0[25] to generate and score 1000 configurations, of which 10% (100) were selected using a buried surface area cutoff of 90% and using energy scoring from Dock4.0, for further analysis. The options used in Dock4.0 are flexible ligand docking with torsion drive and allowing four bumps.

2) The 100 best conformations selected for each ligand from step a) are subjected to all-atom minimization keeping the protein fixed but the ligand movable. The solvation of each of these 100 minimized structures was calculated using the Analytical Volume Generalized Born (AVGB) continuum solvation method[18]. Then the 10 best structures based on the potential energy of the ligand in the protein, were selected from these 100 structures for the next step.

3) Next we optimize the structure of the receptor/ligand complex allowing the structure of the protein to accommodate the ligand. This is essential to identify the optimum conformations for the complex. The all-atom receptor/ligand energy minimization was performed on the 10 structures from the previous step. Using these optimized structures, we calculate the binding energy (BE) using the equation:

$$BE = PE \text{ (ligand in protein)} - PE \text{ (ligand in solvent)} \quad (1)$$

as the difference between the energy of the ligand in the protein and the energy of the ligand in water. The energy of the ligand in water is calculated using DREIDING FF and the SGB or AVGB continuum solvation method[18].

4) Next we select from the five structures from step 3, the one with the maximum number of hydrogen bonds between ligand and protein. For this structure we use the SCREAM side chain replacement program to reassign all side chains for the residues within 5 Å in the binding pocket [this uses a side-chain rotamer library (1478 rotamers with 1.0Å resolution) with the all-atom DREIDING energy function to evaluate the energy for the ligand-protein complex. The binding energy of all the 5 optimized complexes is calculated.

Locating the Putative Binding Site: To locate the binding site of dopamine, other agonists and antagonists, we scanned the entire D_2DR structure without any knowledge of

the binding site. The molecular surface of the entire receptor structure was mapped using autoMS utility of DOCK4.0[25]. Spheres were generated to fill up the void regions of the entire receptor using sphgen utility of Dock4.0. The program "Pass"[26] was then used to locate plausible centers of large void regions in the receptor. The spheres that are within 5.0 Å of these centers are gathered for docking of ligands. For D_2DR we obtained 9 regions where we applied the ScanBindSite protocol for each region, with the following docking steps:

Prediction of binding sites and binding energies: We used HierDock protocol steps a) to d) to dock dopamine to region 1. HierDock protocol steps a) to d) were applied to these regions and the best 5 bound structures for each ligand was chosen.

Refinement of the bound structures: The binding site of the best-bound structures for each ligand was further refined using the following procedure. The docked structures were fully minimized for 5000 steps or 0.1 RMS deviations. Residues in the 5.5 Å vicinity of the ligand were replaced with alanine. Conjugate gradient minimization was carried out for 5000 steps or 0.1 kcal/mol/Å RMS deviations to relax the ligand in the active site. This would allow the ligand to optimize in the putative binding cavity. The side chain rotamers of the residues were replaced using SCREAM side chain placement program and the ligand/receptor complex was again minimized in energy for 5000 conjugate gradient steps or 0.1kcal/mol/Å RMS deviations. The binding energies were calculated suing equation (1).

The final docked conformation of dopamine in the hD_2DR receptor was transferred to the other 4 proteins by aligning the protein backbone and transferring the ligand to the new target. Conjugate gradient minimization was carried out for 5000 steps or 0.1 kcal/mol/Å RMS deviations to relax the ligand in the active site. This would allow the ligand to optimize in the putative binding cavity. The side chain rotamers of the residues were replaced using SCREAM side chain placement program and the ligand/receptor complex was again minimized in energy for 5000 conjugate gradient steps or 0.1kcal/mol/Å RMS deviations. The binding energies were calculated suing equation (1).

The Ballesteros & Weinstein General Indexing Method for Residue Numbering: In order to simplify the comparison of aligned residues in different GPCRs, we will utilize the numbering method of Ballesteros and Weinstein (B&W)[27]. The B&W nomenclature assigns the most conserved residue in each transmembrane segment with an index number of 50. For example, Asn is the most conserved residue in TM1 (this is Asn55 in rhodopsin) and this residue is designated as $Asn^{1.50}$ where 1 stands for the transmembrane helix that the residue belongs to. Based on this nomenclature, the residue immediately before Asn in TM1 is denoted as 1.49 and the residue immediately after is denoted 1.51 et cetera. This method facilitates comparison among different GPCRs by using the most conserved residue in each helix as a reference point. The index residue in each transmembrane segment of rhodopsin is $Asn55^{1.50}$, $Asp83^{2.50}$, $Arg135^{3.50}$, $Trp161^{4.50}$, $Pro215^{5.50}$, $Pro267^{6.50}$, and $Pro303^{7.50}$. All of these residues are 99%-100% conserved in the dopamine systems amongst all organisms and therefore allow unambiguous alignment of the transmembrane of these receptors.

Results and Discussions:

Class I antagonist binding site: A comparison of the D_1like and D_2like clozapine binding sites. Class I antagonists (exemplified by clozapine) occupy the region between TM3, TM4, TM5 and TM6 (the agonist binding pocket). The binding site of clozapine has been previously described for the hD_2DR receptor[1] and is shown in **Figure 5-2**. In its bound conformation, clozapine forms a 2.8 Å salt bridge to Asp114 (3.32); a single hydrogen bond to Ser193 (5.42) (3.2 Å) (but not to Ser194 (5.43) or Ser197 (5.46)); heteroatom interactions with Trp386 (6.48) (3.1 Å); and, residues Val87 (2.57), Trp90 (2.60), Phe110 (3.28), Leu113 (3.31), Vall115 (3.33), Met117 (3.35), Cys118 (3.36), Phe164 (4.54), Phe189 (5.38), Val190 (5.39), Ser194 (5.33), Ser197 (5.36), Phe382 (6.44), Trp386 (6.48), Phe389 (6.51), Phe390 (6.52), Thr412 (7.39), Trp413 (7.40), Tyr416 (7.43), and Ser419 (7.46) create a mostly hydrophobic pocket for the multiple ring system of the ligand. Clozapine interacts with residues at similar positions in the D_1like subtypes of the dopamine receptors (see **appendices III and VI**).

Herein, we highlight the differences in the Clozapine binding sites to the D_1 and D_2like systems. The most important modifications occur at positions 3.28, 3.31, 3.35, 3.36, 3.39, 4.54, 4.58, 5.37, 5.38, 5.41, 6.55, 6.56, and 7.39.

Major changes in TM3 include a tryptophan (D_1like) to phenylalanine (D_2like) transition at position 3.28. The presence of the indole ring of tryptophan causes the TM3 aspartate to form an interaction with the ring and a second interaction with the amino group of the ligand. A second profound change for receptor specificity occurs at position

3.31. In the D_1like receptors, the 3.31 position is a bulky phenylalanine residue; in the D_2like receptors, this phenylalanine is replaced with smaller hydrophobic amino acid such as leucine (D_2). The presence of the phenylalanine residue at position 3.31 helps stabilize the class I antagonists such as clozpaine, but it blocks access into the void between TM2 and 7 utilized by the larger class II antagonists such as haloperidol. The last set of modifications in TM3 occur at positions 3.35, 3.36 and 3.40 where in the D_1like receptors a cysteine (3.35), and a pair of serines (3.36 and 3.40) create a large polar cavity with the ability to donate and accept multiple strong hydrogen bonds. At similar positions in the D_2like receptors, a methionine (3.35) a cysteine (3.36), and serine (3.40) create a more restricted and less polar cavity with reduced hydrogen bonding ability.

Two interesting changes occur at positions 4.54 and 4.58 in TM4 of dopamine receptors. The first aromatic microdomain, described previously, consists of residues at positions 4.50 and 4.54; in the hD_2DR, a Trp and a Phe occupy these positions, respectively. A Phe to Val transition at position 4.54 of the D_1like receptors creates a larger cavity for the D_1like receptors that could readily accommodate ligands with multiple ring systems; these large ligands are unlikely to be accommodated in the D_2like receptors due to the presence of the bulkier aromatic at position 4.54. Position 4.58 is the second of the variable regions within the class I antagonist binding cavity. In the D_1like receptors, a large bulky Phe residue occupies position 4.58; a smaller and significantly more polar Cys residue in the D_2like receptors occupies the same position. The combination of the two fine, yet important differences in the structures could be utilized

to create receptor specific drugs by taking advantage of the change in hydrogen bonding potential, polarity and size of the cavity in the vicinity of TM4.

Three modifications at positions 5.37, 5.38, 5.41 appear to be important in ligand recognition and differentiation between different receptor subtypes. Position 5.37 harbors a Thr (D_1like) to Ala (D_2like) transition; this modification causes a clear difference in polarity/hydrogen bonding, and a minor difference in size in the TM5 domain. Position 5.38 shows a Tyr (D_1like) to Phe (D_2like) transition; although the difference in size between the tyrosine and phenylalanine residues is insignificant, the transition allows for an additional unit of hydrogen bonding and increased polarity in the cavity of the D_1like receptors. A major difference in TM5 between the D_1like and D_2like receptors is in the number of serine residues present in this transmembrane helix; the D_1like receptors have a total of 4 serines in TM5, but the D_2like receptors have only 3 serines. A third significant modification in TM5 occurs at position 5.41 where the fourth serine is introduced in the D_1like receptors; a Tyr residue in the D2like receptors occupies position 5.41. The modifications at positions 5.37, 5.38, 5.41 cause the D_1like receptor to be significantly more polar at the 5th transmembrane domain.

Positions 6.55 and 6.56 are the important points of modification in TM6. Similar to the β_2 adrenergic receptor, the D_1like receptors have an Asn residue at position 6.55; the D_2like receptors have a His residue at the same position. The Asn to His transition provides for differences in polarity and hydrogen bonding capabilities at this position.

Residue 6.56 exasperates the differences in polarity between the two classes of receptors; in the D_1like receptors, 6.56 is a Cys, in the D_2like receptors this position is an Ile.

TM7 shows a single difference at position 7.39 where a valine (D_1like) to threonine (D_2like) modification causes increased polarity for the D_2like receptors.

In general, the combination of the changes in TM3, 4, 5 and 6 create a larger and more polar cavity in the D_1like receptors that would better accommodate polar polycyclic ligands.

Class I antagonist binding site: A comparison of the D_1 and D_5 clozapine binding sites.
In the vicinity of the binding site, there are few transmembrane residues that are different between the receptors (**Figure 5-3**). A possible culprit in causing differential binding would be the second extracellular loop, which shows the greatest variability between the two-receptor sequences. Currently, our modeling procedure is not efficient at predicting structures with the closed loop.

Class I antagonist binding site: A comparison of the D_2 and D_3 clozapine binding sites.
As is the case with the dopamine-binding site, there is no difference in the residues present in the D_2 versus the D_3 class I antagonist-binding sites (**Figure 5-4**). Both D_2 and D_3, with 76% sequence identity, share identical class I antagonist-binding sites as exemplified by the clozapine binding site. Again, a similar line of reasoning as for the

agonist binding site would lead one to hypothesize that the second extracellular loop will play the most direct role in subtype selectivity and differentiation between ligands.

Class I antagonist binding site: A comparison of the D_2 and D_4 clozapine binding sites. There are significant differences between the class I antagonist-binding sites of the D_2 and D_4 receptors (**Figure 5-5**). Positions 2.60, 3.28, 3.31, 3.35, 4.54, 4.58, and 5.38 are variable regions between the D_2 and D_4 proteins.

Although clozapine is a class I antagonist, meaning it mainly occupies the void between TM3 and 6 with minimal contacts to TM4 and 5, one TM2 residue, 2.60, does appear in the binding cavity of Clozapine. Position 2.60 is a Trp in D_2 and a Leu in D_4. Several groups[28] have shown that residues in TM2 are responsible for the differential binding of ligands to the D_2 and D_4 receptors.

Position 3.28 is an important site of differentiation between the two receptors. The aromatic residue, one turn of the helix above the TM3 conserved aspartate, is mutated to a non-aromatic Leu111 in the D_4 receptor. The aromatic to aliphatic transition at position 3.28 creates a less rigid and spacious cavity in the D_4 receptor and removes the possibility of a stabilizing cation-pi interaction. Position 3.31 (Leu in D_2 and Met in D_4) also exhibits minor differences in size and polarity between the two receptors. Again, the nature of the modification is similar, although the methionine is slightly more polar. Position 3.35 shows a similar modification as the methionine one turn of the helix below the aspartate in D_2 has been mutated to a leucine in D_4; not a major chemical change, although the

methionine is a more linear amino acid and could potentially allow a larger ligand to occupy the cavity. All three changes in TM3 replace amino acids with others of similar hydrophobic character, but the D_4 receptor appears to have a less rigid and more spacious cavity for ligand binding.

Positions 4.54 and 4.58 are important variable regions between the D_2 and D_4 receptors. Two transitions, a Phe to Ala and a Cys to Ala, provide the D_4 receptor with a larger and less polar cavity in the vicinity of TM4.

TM5 shows one minor, but potentially useful difference at position 5.38 where a Phe to Tyr transition allows for added hydrogen bonding capability in the D_4 receptor.

Despite the rich degree of variation in TM3, 4, and 5, TM6 and 7 exhibit no differences in the class I antagonist binding sites.

Class II antagonist binding site: A comparison of the D_1like and D_2like haloperidol binding sites. Class II antagonists, exemplified by haloperidol, occupy the region between TM2, TM3, TM6, TM7 with minimal contacts to TM4 and TM5 (**Figure 5-6**). Haloperidol, for example, makes a 2.8 Å salt bridge to Asp114 (3.32); hydrogen bond (3.2 Å) to Ser197 (5.46) (3.2 Å) (but not to Ser193 (5.42) or Ser194 (5.43)); heteroatom interactions with Trp386 (6.48) at 3.8 Å and Trp90 (2.60) at 3.0 Å; and, residues Val87 (2.57), Val91 (2.61) and Leu94 (2.64), Phe110 (3.28), Leu113 (3.31), Val115 (3.33), Met117 (3.35), and Cys118 (3.36), Trp160 (4.50), Phe164 (4.54), Phe189 (5.38), Val190

(5.39), Val196 (5.45), Trp386 (6.48), Phe389 (6.51), Phe390 (6.52), and His393 (6.55), Ser409 (7.36), Thr412 (7.39), Trp413 (7.40), Tyr416 (7.43), and Val417 (7.44) provide a mostly hydrophobic pocket for the ligand. Other class II antagonists with very similar binding sites include spiperone and sulpiride.

Class II antagonists are predicted and are shown experimentally to preferentially bind to the D_2like receptors. This experimentally and theoretically observed preference is predicted to be due to the presence of a phenylalanine, at position 3.31 in the D_1like sequences. This phenylalanine, which is, conserved between the D_1 and D_5 receptors, blocks the cavity for the long ligands to extend into the second aromatic microdomain of the dopamine receptors located between TM2 and 7. Should a longer ligand extend into the second aromatic micro-domain, there is significant variability in the region between TM1, 2 and 7. Based on this observation, the only variability present is in the region constituting the class I antagonist binding site (i.e., positions 3.28, 3.31, 3.35, 3.36, 3.39, 4.54, 4.58, 5.37, 5.38, 5.41, 6.55, 6.56, and 7.39), which has been previously discussed extensively.

Class II antagonist binding site: A comparison of the D_1 and D_5 haloperidol binding sites. Class II antagonists do not bind well to the D_1like receptors, meaning they will have mediocre binding to both D_1 and D_5 subtypes of the human dopamine receptors (**Figure 5-7**). As mentioned previously, there is no difference in the dopamine and class I antagonist binding sites of either receptor. Since the class II antagonists cannot penetrate into the TM1, 2, and 7 domains, and are restricted to the class I antagonist site, they will also have similar binding sites between the D_1 and D_5 receptors. There is only one amino

acid difference in the binding site between the D_1 and D_5 receptors. This amino acid difference is in TM4 position 4.54, where a valine to isoleucine mutation has occurred between the D_1 and D_5 receptors. This difference is not significant, nor useful considering this class of antagonists does not bind well to these receptors.

Class II antagonist binding site: A comparison of the D_2 and D_3 haloperidol binding sites. The D_2 and D_3 class II antagonist binding sites are identical (**Figure 5-8**). This is clearly illustrated by the fact that most class II antagonists show similar binding affinities to D_2 and D_3 receptors. Recently, some receptor specific antagonists have been synthesized, but differential binding has been attributed to the interaction with loop residues near the extracellular domains. We reproduce the experimental observation of similar binding between the D_2 and D_3 receptor, but using a TM only analysis; we are unable to define the nature of differential binding of the more specific ligands.

Class II antagonist binding site: A comparison of the D_2 and D_4 haloperidol binding sites. There are many points of differentiation between the D_2 and D_4 class II antagonist binding sites (**Figure 5-9**). The binding site is located between the voids of TM2, 3, 4, 5, 6, and 7. The major positions of modification are at points 2.60, 2.61, 2.64, 3.28, 3.31, 3.35, 3.36, 3.39,

There are three modifications in TM2: 1) a Trp to Leu transition between D_2 and D_4 at position 2.60; 2) a Lys to Phe transition at 2.61; and 3) a Val to Ser transition at 2.64. Both transitions can account for differential binding of ligands to this receptor. The

serine in TM2 of D_4 can be used in binding ligands with heteroatom modifications on the aromatic ring binding in the second aromatic microdomain. The tryptophan to leucine modification expands the cavity, allowing for larger ligands to occupy the site, and the Lys to Phe modification could be used in design of anionic antagonists.

The TM3 modifications (positions 3.28, 3.31, 3.35, 3.36, 3.39) have been previously discussed. The modification of the aromatic at position 3.28 to leucine removes a possibly important cation-pi interaction; it also creates a larger cavity for the ligand to bind. Furthermore, whereas the aromatic residue usually caps the cavity and does not allow the ligand to extend towards the extracellular, the leucine cannot effectively cap the cavity and the ligand may adopt alternative conformations. The remainder of the residues in TM3 are simple modifications that do not drastically change the nature of the cavity.

There is a single change in TM4 at position 4.54 where the phenylalanine of the first aromatic micro-domain in D_2 has been mutated to an alanine in D_4, thereby removing its ability to stabilize the ligand. This modification causes an enlargement of the cavity. The TM2, 3, and 4 modifications, all cause an enlargement of the binding cavity, allowing for a larger ligand to occupy the site. There are no appreciable differences in the residues facing the binding cavity in the remaining helices of the bundle.

Conclusion:

Modifications in the transmembrane helices cause differential binding of ligands to the 5 subtypes of the human dopamine receptors. The transmembrane mutations can be used to identify the mechanism of differentiation and in designing receptor specific ligands. We have identified residues in the binding sites of agonists, class I antagonists, and class II antagonists for all 5 subtypes of the human dopamine receptor and identified points of difference that may be used by medicinal chemists in design and synthesis of receptor and subtype specific ligands. Most importantly, 1) modifications in TM2 are important for D_2-D_4 selectivity, 2) variations in TM1 are rarely taken advantage of in the design of aminergic ligands, and 3) modifications of TM3 are important for D_1like-D_2like specificity. Selectivity between D_1-D_5 and D_2-D_3 most likely involved the EC2 loop and requires detailed studies of the loop structure connecting TM4 and TM5.

Figures:

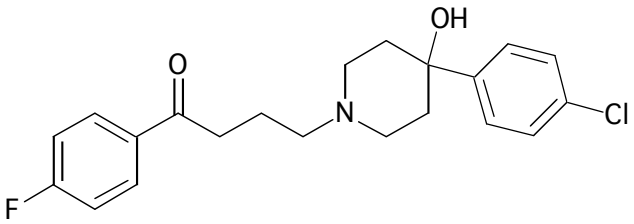

Haloperidol

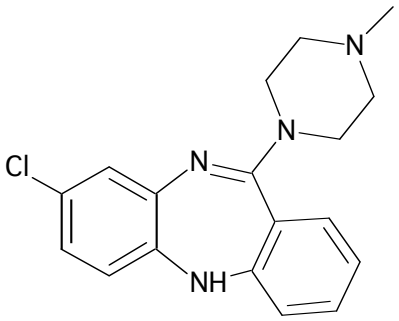

Clozapine

Figure 5-1. The structure of haloperidol and clozapine, two antagonists of the human dopamine receptors.

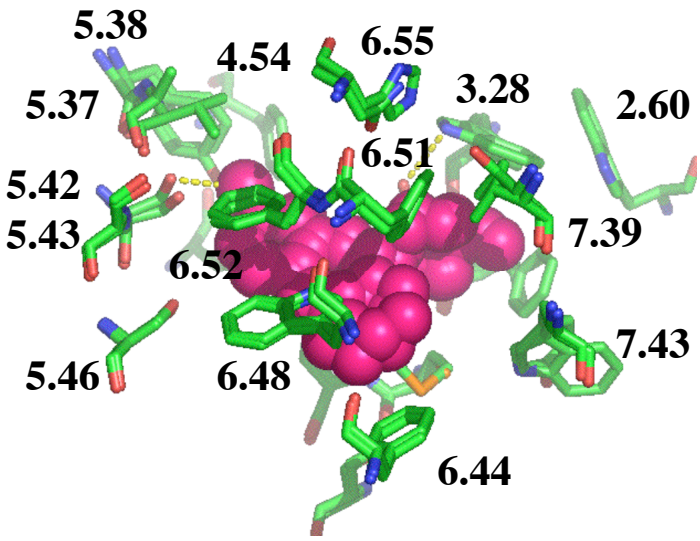

Figure 5-2. An overlay of the class I antagonist binding site of clozapine to the D_1 and the D_2 subtypes of the human dopamine receptors. Residues are numbered according to the Ballesteros and Weinstein indexing nomenclature, where the first number represents the transmembrane helix to which the residue belongs to, and the two digit number corresponds to the residue position with respect to the most conserved residue in each helix. Positions 3.28, 3.31, 4.54, 5.37, 5.38, 5.41, 6.55, 6.56, 7.39 and 7.43 in the Clozapine binding site are variable between the D_1like and D_2like receptors. The combination of these modifications causes differential binding of ligands to these two families of dopamine receptors.

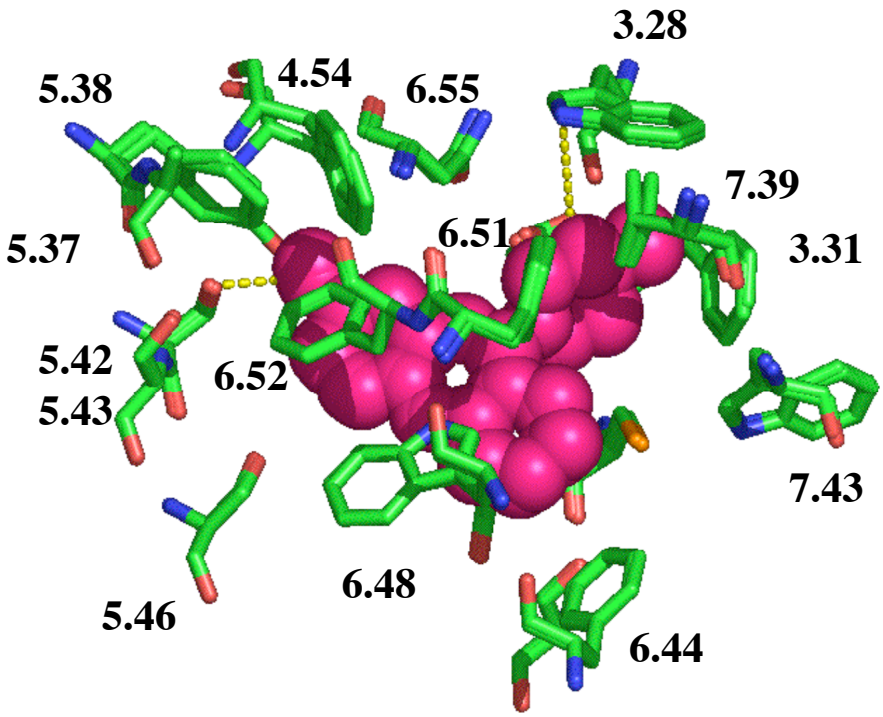

Figure 5-3. An overlay of the class I antagonist binding site of clozapine to the D_1 and the D_5 subtypes of the human dopamine receptors. Notice that there are no differences in the transmembrane helices that make up the binding sites of these subtypes. Both receptors have similar binding affinities for ligands. Minor differences in binding affinity may be caused by the second extracellular loop.

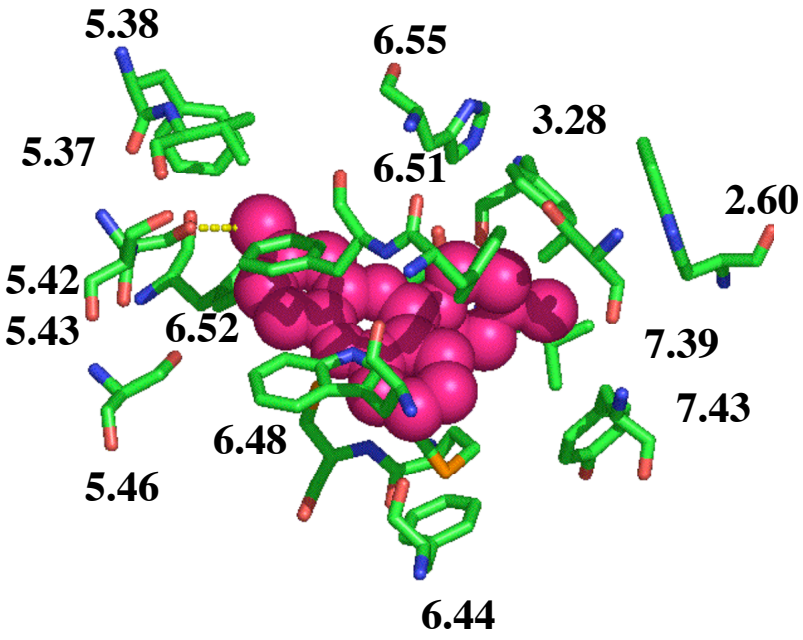

Figure 5-4. An overlay of the class I antagonist binding site of clozapine to the D_2 versus the D_3 subtypes of the human dopamine receptors. Notice that there are no differences in the transmembrane helices that make up the binding sites of these subtypes. Differences in binding affinity may be caused by the second extracellular loop.

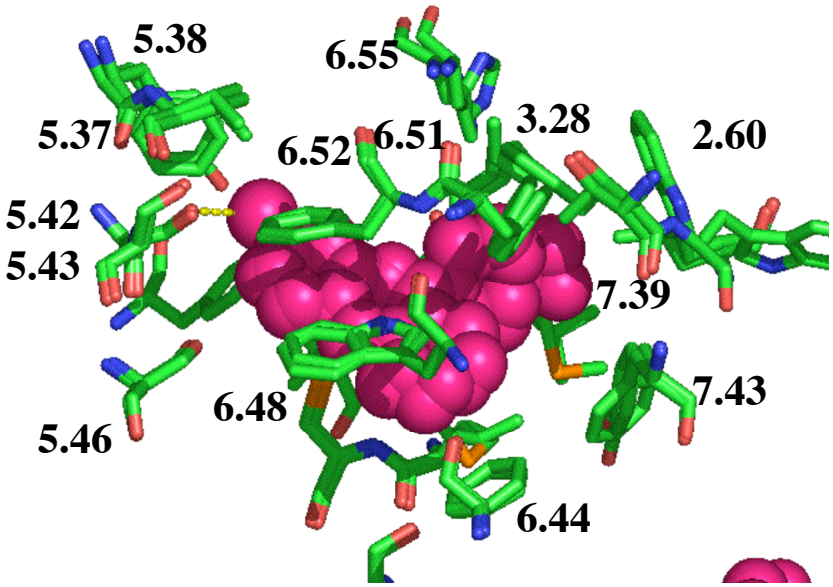

Figure 5-5. An overlay of the class I antagonist binding site of clozapine to the D_2 versus the D_4 subtypes of the human dopamine receptors. Positions 2.60, 3.28, 3.31, 3.35, 4.54, 4.58, and 5.38 are variable regions between the D_2 and D_4 proteins.

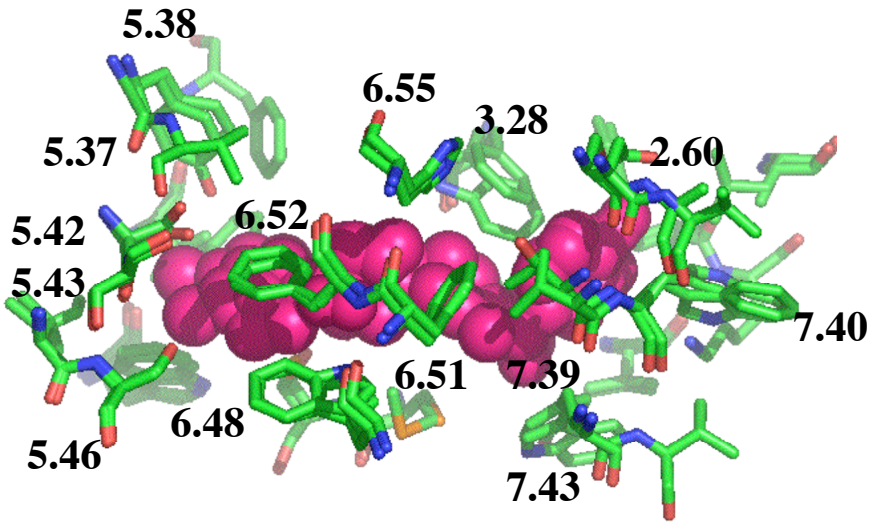

Figure 5-6. An overlay of the class II antagonist-binding site of haloperidol to the D_1like versus the D_2like subtypes of the human dopamine receptors. Haloperidol and other class II antagonists have a low affinity for the D_1like subtypes of the human dopamine receptors due to the presence of a Phe residue at position 3.31 that blocks access to the cavity between TM2 and 7.

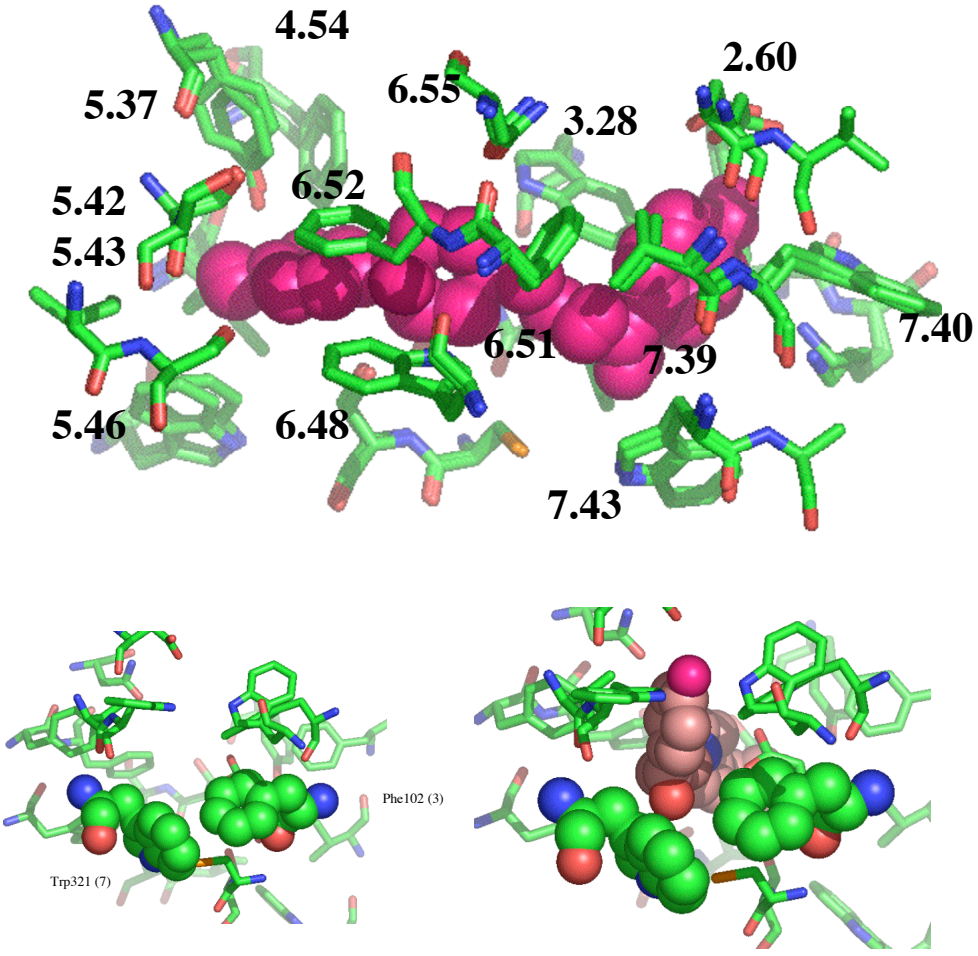

Figure 5-7. An overlay of the class II antagonist-binding site of haloperidol to the D_1 and the D_5 subtypes of the human dopamine receptors. Notice that there are no differences in the transmembrane helices that make up the binding sites of these subtypes. Both receptors have similar binding affinities for ligands. Minor differences in binding affinity may be caused by the second extracellular loop. The presence of a Phe residue at the 3.31 position blocks the cavity between TM2 and 7 causing class II antagonists to have a low affinity for the D_1 and D_5 receptors.

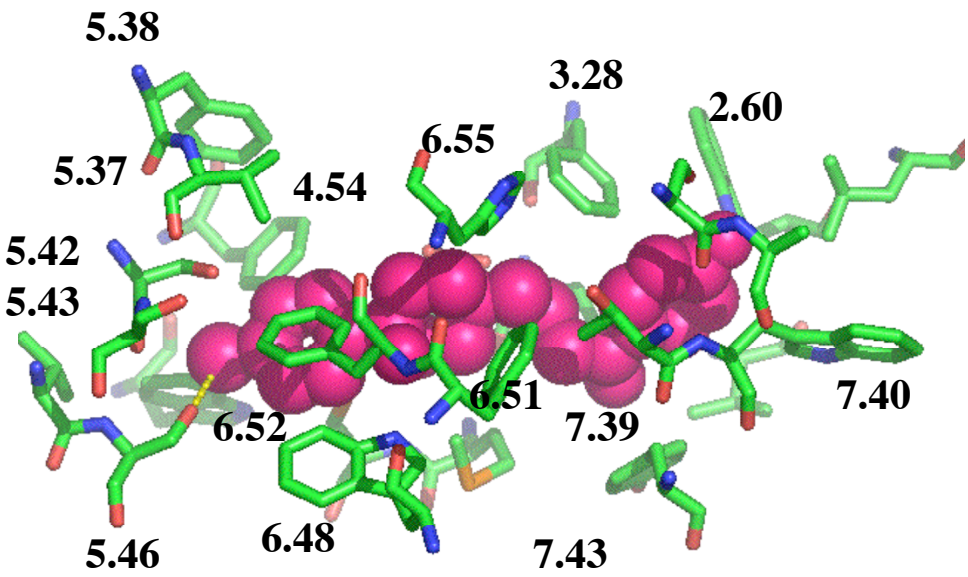

Figure 5-8. An overlay of the class II antagonist-binding sites of haloperidol to the D_2 and D_3 binding sites to the human dopamine receptors. Notice that there are no differences in the transmembrane helices that make up the binding sites of these subtypes. Differences in binding affinity may be caused by the second extracellular loop.

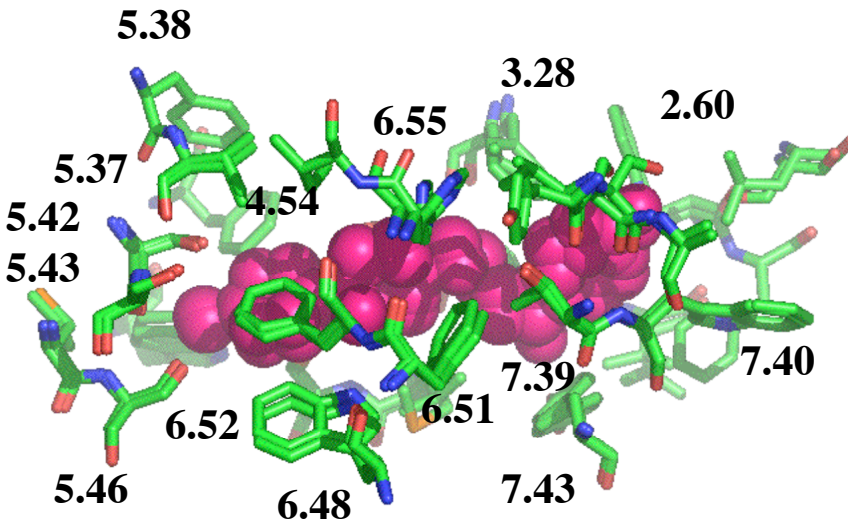

Figure 5-9. An overlay of the class II antagonist binding sites of haloperidol to the D_2 and the D_4 subtypes of the human dopamine receptors. Major differences between the two subtypes are present in the TM2 and TM7 boundary where position 2.60 in the D_2 receptor has been mutated from an aromatic residue to aliphatic residue increasing cavity size in the D_4 receptor.

MDPLNLSWYDDDLERQNWSRPFNGSDGKADRPHYNYYATLLTLLIAVIVFGNV
LVCMAVSREKALQTTTNYLIVSLAVADLLVATLVMPWVVYLEVVGEWKFSRIH
CDIFVTLDVMMCTASILNLCAISIDRYTAVAMPMLYNTRYSSKRRVTVMISIVWV
LSFTISCPLLFGLNNADQNECIIANPAFVVYSSIVSFYVPFIVTLLVYIKIYIVLRRRR
KRVNTKRSSRAFRAHLRAPLKGNCTHPEDMKLCTVIMKSNGSFPVNRRRVEAAR
RAQELEMEMLSSTSPPERTRYSPIPPSHHQLTLPDPSHHGLHSTPDSPAKPEKNGH
AKDHPKIAKIFEIQTMPNGKTRTSLKTMSRRKLSQQKEKKATQMLAIVLGVFIIC
WLPFFITHILNIHCDCNIPPVLYSAFTWLGYVNSAVNPIIYTTFNIEFRKAFLKILHC

Scheme 5-1. The predicted transmembrane regions of the human D_2 dopamine receptor. Residues in red correspond to the transmembrane helices, while the residues in black represent the N & C termini, and the loops connecting the transmembrane domains.

References:

[1] Kalani M.Y., Vaidehi N., Hall S.E., Trabanino R., Freddolino P., Kalani M.A., Floriano W.B., Kam V., Goddard W.A., III *Proc. Natl. Acad. Sci. USA* 101, 3815-3820 (**2004**).

[2] Jackson D. M., Westlind-Danielsson A. *Pharmacol. Ther.* 64, 291-369 (**1994**).

[3] Strange P.G. *Adv. Drug Res*. 28, 313-351 (**1996**).

[4] Missale C., Nash S. R., Robinson S. W., Jaber M., Caron M.G. *Physiol. Rev.* 78, 189-225 (**1998**).

[5] Kobilka B.K., Kobilka T.S., Daniel K. *Science* 240, 1310 (**1988**).

[6] Palczewski K., Kumasaka T., Hori T., Behnke C. A., Motoshima H., Fox B. A., Le Trong I., Teller D. C., Okada T., Stenkamp R. E. *Science* 289**,** 739–745 (**2000**).

[7] (a) Teeter M.M., Froimowitz M., Stec B., DuRand C.J. *J. Med. Chem* . 37, 2874-2888 (**1994**). (b) Trumpp-Kallmeyer S., Hoflack J., Bruinvels A., Hibert M. *J. Med. Chem.* 35, 3448-3462 (**1992**).

[8] (a) Neve K.A., Cumbay M.G., Thompson K.R., Yang R., Buck D.C., Watts V.J., DuRand C.J., Teeter M.M. *Mol. Pharmacol*. 60, 373-381 (**2001**). (b) Varady J., Wu X., Fang X., Min J., Hu Z., Levant B., Wang S. *J. Med. Chem*. 46, 4377-4392 (**2003**).

[9] (a) Vaidehi N., Floriano W., Trabanino R., Hall S., Freddolino P., Choi E.J., Zamanakos G., Goddard, W.A. *Proc. Natl. Acad. Sci. U.S.A.* 99, 12622-12627 (**2002**). (b) Trabanino R., Hall S.E., Vaidehi N., Floriano W., Goddard, W.A. *Biophys. J.*, in press (**2004**).

[10] Freddolino P., Kalani M.Y., Vaidehi N., Floriano W., Hall S.E., Trabanino R., Kam V.W.T., Goddard, W.A. *Proc. Natl. Acad. Sci. U.S.A.* 101, 2736-2741 (**2004**).

[11] (a) Floriano W. B., Vaidehi N., Goddard W. A., III, Singer M. S., Shepherd G. M. *Proc*. *Natl*. *Acad*. *Sci*. *U.S.A.* 97**,** 10712–10716 (**2000**). (b) Floriano W.B. Vaidehi N., Goddard W.A., III, *Chemical Senses*, in press (**2004**). (c) Hall S.E., Vaidehi N., Floriano W.B., Goddard W.A., III, *Chemical Senses*, in press (**2004**).

[12] Mayo S. L., Olafson B.D., Goddard III, W.A. *J. Phys. Chem.* 94, 8897-8909 (**1990**).

[13] Sali A., Potterton L., Yuan F., van Vlijmen H., Karplus M. *Proteins* 23**,** 318 (**1995**).

[14] Ding H. Q., Karasawa N., Goddard III, W. A. *J. Chem. Phys.* 97, 4309 (**1992**).

[15] Lim K-T, Brunett S., Iotov M., McClurg R.B., Vaidehi N., Dasgupta S., Taylor S., Goddard III, W.A. *J. Comput. Chem.* 18, 501-521 (**1997**).

[16] Gasteiger J., Marsili M. *Tetrahedron* 36, 3219-3228 (**1980**).

[17] Rappé A.K., Goddard III, W.A. *J. Phys. Chem.* 95, 3358-3363 (**1991**).

[18] Zamanakos G., Physics Doctoral Thesis, California Institute of Technology, (**2001**).

[19] Higgins D., Thompson J., Gibson T., Thompson J.D., Higgins D.G., Gibson T.J. *Nucleic Acids Res.* 22, 4673-4680 (**1994**).

[20] Schertler G.F.X. *Eye* 12, 504-510 (**1998**).

[21] (a) Jain A., Vaidehi N., Rodriguez G. *J. Comp. Phys.* 106, 258-268 (**1993**). (b) Vaidehi N., Jain A., Goddard III, W.A. *J. Phys. Chem.* 100, 10508-10517 (**1996**).

[22] Vriend G. *J. Mol. Graph.* 8, 52-56 (**1990**).

[23] Datta D., Vaidehi N., Floriano W. B., Kim K. S., Prasadarao N. V., Goddard W. A., III *Proteins Struct. Funct. Genet.* 50**,** 213–221 (**2003**).

[24] (a) Zhang D., Vaidehi N., Goddard W. A., III, Danzer J. F., Debe D. *Proc. Natl. Acad. Sci. U.S.A.* 99**,** 6579–6584 (**2002**). (b) Wang P., Vaidehi N., Tirrell D. A., Goddard W. A., III *J. Am. Chem. Soc.* 124**,** 14442–14449 (**2002**). (c) Kekenes-Huskey P. M., Vaidehi N., Floriano W. B., Goddard W. A., III *J. Phys. Chem. B* 107**,** 11549–11557 (**2003**). (d) Floriano W. B., Vaidehi N., Zamanakos G., Goddard W. A., III *J. Med. Chem.* 47**,** 56–71 (**2004**).

[25] Ewing T.A., Kuntz I.D. *J. Comput. Chem.* 18, 1175-1189 (**1997**).

[26] Brady P., Stouten F.W. *J. Comp. Molec. Des.* 14, 383-401 (**2000**).

[27] Ballesteros J., Weinstein H. *Methods Neurosci*. 25, 366-428 (**1995**).

[28] (a) Simpson M.M., Ballesteros J.A., Chiappa V., Chen J., Suehiro M., Javitch J. *Mol. Pharmacol.* 56, 1116-1126 (**1999**). (b) Schetz J.A., Benjamin P.S., Sibley D.R. *Mol. Pharmacol.* 57, 144-152 (**2000**).